Infrared Physics & Technology 69 (2015) 238–243

Contents lists available at ScienceDirect

Infrared Physics & Technology

journal homepage: www.elsevier.com/locate/infrared

The use of infrared self-emission measurements to retrieve surface temperature of levitating water droplets

Alexander A. Fedorets [a], Leonid A. Dombrovsky [b,*], Andrey M. Smirnov [c]

[a] Tyumen State University, Semakov 10, Tyumen 625003, Russia
[b] Joint Institute for High Temperatures, NCHMT, Krasnokazarmennaya 17A, Moscow 111116, Russia
[c] JSC NPP Pulsar, Okruzhnoy proezd 27, Moscow 105187, Russia

HIGHLIGHTS

- Surface temperature of droplets levitating above a hot water layer is determined.
- The apparent temperature was measured in the infrared absorption band.
- Angular dependences of spectral emittance were used to retrieve the temperature.
- Spectral sensitivity of camera and optical filter are taken into account.

ARTICLE INFO

Article history:
Received 20 January 2015
Available online 4 March 2015

Keywords:
Levitation
Cluster of droplets
Infrared range
Absorption band
Microscopic measurements
Temperature profile

ABSTRACT

Levitating small water droplets formed from the upward flow of steam and entrained air above the heated water surface are studied. The case of relatively large droplets in the middle of a droplet cluster which is practically immobile at a small distance from the water surface is considered. The close-up infrared measurements in the spectral absorption band of water are used to identify temperature of the upper surface of the droplet. Both the directional spectral emittance of water surface and the spectral sensitivity of the device are taken into account to formulate an inverse problem for the integral equation. The numerical solution of this problem showed that temperature is minimal at the top of droplet and increases sharply towards the droplet equator. This temperature difference increases almost linearly with the droplet size. The results obtained are expected to be useful for more detailed physical analysis and possible modeling of complex behavior of the levitating droplet clusters.

1. Introduction

The levitating droplets which form relatively stable clusters above the heated water surface were originally observed by Fedorets [1] more than ten years ago. Typical clusters of water droplets are shown in Fig. 1. The behavior of the levitating single droplets and droplet clusters in the upcoming flow of vapor of various liquids and entrained air above the heated surface of the liquid has been studied experimentally in several papers [2–6] and this problem remains interesting up to now for researchers from different countries [7,8]. Nevertheless, there is no reliable information on temperature of levitating droplets at the moment. This problem is partially solved in the present paper by using fine infrared measurements for the specific case of relatively large water droplets. The results obtained are important to develop adequate physical and computational models of this phenomenon.

2. Infrared radiation of water droplets

The infrared radiation emitted by a single homogeneous spherical particle of arbitrary size can be calculated on the basis of the rigorous Lorenz–Mie theory or simply Mie theory [9–11]. There are only two independent dimensionless variables in Mie solution: (1) the diffraction parameter $x = 2\pi a/\lambda$, where a is the particle radius and λ is the radiation wavelength and (2) the complex index of refraction $m = n - i\kappa$, where n is the index of refraction and κ is the index of absorption. A lot of papers with numerical data concerning optical properties of various particles have been published with appearance of modern computers. The reader can just refer to monographs [12–17], where one can find not only a theoretical and

* Corresponding author. Tel.: +7 499 250 3264.
E-mail address: ldombr@yandex.ru (L.A. Dombrovsky).

http://dx.doi.org/10.1016/j.infrared.2015.02.005
1350-4495/

Nomenclature

a	droplet radius
B	Planck's function
F	transmittance of filter
x	diffraction parameter
n	index of refraction
q	radiative flux
r	current radius
T	temperature
y	coordinate along the cluster diameter
z	coordinate along the droplet diameter

Greek symbols

α	absorption coefficient
δ	thickness of radiating layer
ε	emittance
κ	index of absorption
λ	wavelength of radiation
μ	directional cosine
θ	polar angle
ρ	phase shift
τ	optical thickness
Φ	spectral sensitivity of camera

Subscripts

b	brightness
d	droplet
m	measured
n	normal
s	surface
λ	spectral

computational analysis of the problem but also some particular data for various particles of different substances.

The levitating water droplets considered in the present paper are usually much greater in size than the wavelength. This statement is usually true not only for almost monodisperse droplets in the central region of droplet clusters but also for slightly smaller droplets at the cluster periphery. It means that one can use the geometrical optics approximation instead of the Mie theory. The geometrical optics (ray optics) is correct for large particles at a large phase shift [13,17–21]:

$$x \gg 1 \quad \rho = 2x(n-1) \gg 1 \tag{1}$$

The last condition is important because large particles of optically "soft" substance are in the range of anomalous diffraction, where interference of transmitted and diffracted radiation is considerable [17]. It is also clear that geometrical optics approximation is inapplicable for calculations of scattering at special (caustic) angles, where wave effects are important (for rainbow and glory). But this limitation is not directly related to the thermal radiation of particles.

The spectral optical constants, n and κ, of pure water in a wide spectral range are well known [22,23]. Therefore, it can be easily shown that the second of conditions (1) is satisfied for large water droplets in the short-wave part of the infrared spectral range. For convenience of subsequent analysis, the spectral dependences of both the index of refraction and index of absorption are presented in Fig. 2.

In the case of microscopic measurements from the upper side of the levitating droplet, one should use a spectral range where the droplet is opaque and there is no effect of the transmitted radiation from the surface of water layer under the droplet. Fig. 2a indicates that absorption band at $\lambda \approx 3$ μm is the best choice. In fact, the characteristic optical thickness of a droplet is calculated as follows:

$$\tau_\lambda = 2\kappa x = \alpha_\lambda a \quad \alpha_\lambda = 4\pi\kappa/\lambda \tag{2}$$

where α_λ is the spectral absorption coefficient of water [24]. Obviously, the condition $\tau_\lambda \gg 1$ leads to the following inequality for the droplet radius at the above mentioned absorption band with an average value of $\kappa = 0.1$–0.2:

$$a \gg 2\ \mu\text{m} \tag{3}$$

This condition is usually true for the levitating droplets. It is questionable only for the smallest droplets which radius is about 10 μm [25]. One can easily estimate the thickness of a radiating surface layer, δ, of a droplet by using the two-flux approximation [17]:

$$\delta = \frac{1}{2\alpha_\lambda} \approx 1\ \mu\text{m} \ll a \tag{4}$$

It means that the problem really degenerates and the surface radiation of a droplet is observed at the absorption band.

One should recall that the use of infrared measurements in the range of water semi-transparency as it was done in [6] leads to serious difficulties and it is practically impossible to treat the

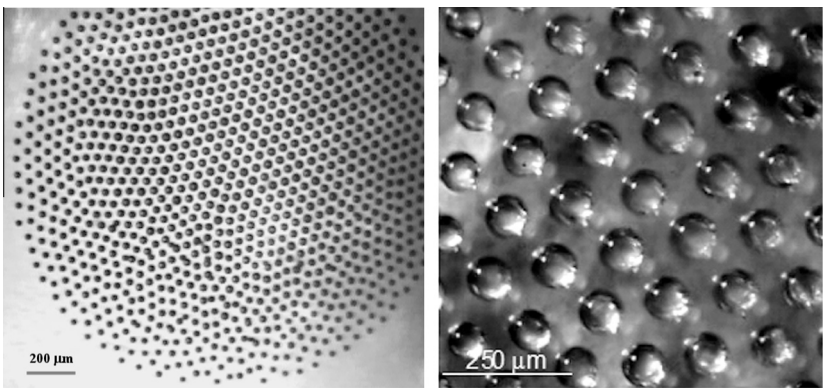

Fig. 1. Typical top views of different clusters of levitating water droplets.

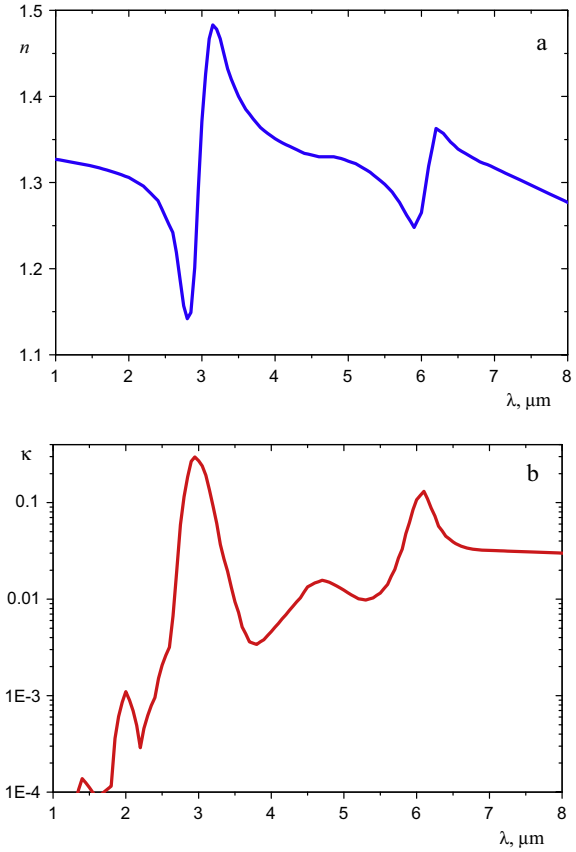

Fig. 2. Indices of (a) refraction and (b) absorption of pure water.

experimental results on infrared radiation in terms of temperature. The latter is related not only with the effect of transmitted thermal radiation from the water layer under the droplet. It is also important that thermal radiation of large semi-transparent particles is emitted mainly from their central region $\bar{r} = r/a < 1/n$. This effect studied in papers [20,26,27] is explained by the total internal reflection of radiation emitted by elementary volumes placed at $\bar{r} > 1/n$ in a part of the whole angle range. Note that this physical effect appeared to be important in several engineering problems related with infrared radiation of particles [28–31] (see [17,32] for more details).

The directional dependence of water surface emittance in the opacity range can be calculated as follows [33,34]:

$$\varepsilon_\lambda(\mu) = 1 - \frac{1}{2}\left[\left(\frac{n^2\mu - \sqrt{n^2-1+\mu^2}}{n^2\mu + \sqrt{n^2-1+\mu^2}}\right)^2 + \left(\frac{\mu - \sqrt{n^2-1+\mu^2}}{\mu + \sqrt{n^2-1+\mu^2}}\right)^2\right]$$
$$\mu = \cos\theta \qquad (5)$$

where θ is the polar angle measured from the normal direction. Strictly speaking, Eq. (5) is correct for dielectrics when $\kappa^2 \ll n^2$ but this condition is also satisfied for water in the infrared spectral range under consideration. The known expression for the normal emittance in a particular case of Eq. (5) at $\theta = 0$ is:

$$\varepsilon_{\lambda,n} = 4n/(n+1)^2 \qquad (6)$$

Fig. 3 shows the directional emittance of water surface at wavelength $\lambda = 3$ μm calculated using Eq. (5). It should be noted that the formal use of the geometrical optics approximation for spherical droplets in the region of a–r comparable or less than λ is incorrect and leads to physically wrong results. The wave effects related with interference of the so-called surface waves with the diffracted

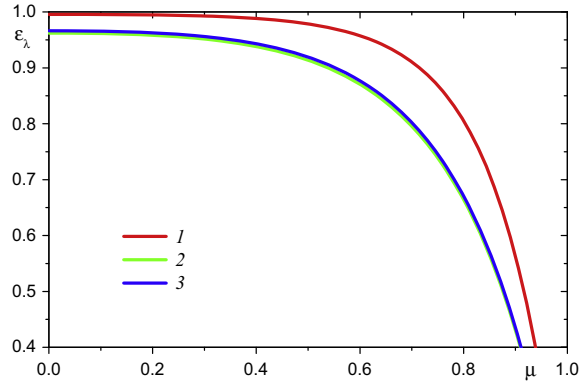

Fig. 3. Calculated directional spectral emittance of water surface: 1 – $\lambda = 2.8$ μm, 2 – 3 μm, 3 – 3.3 μm.

radiation coming from the surface of water layer under the droplet should be taken into account in this region [15]. A similar quantitative limitation of the minimum value of a–r is related with the partial transparency of a thin water layer of thickness δ estimated by Eq. (4). Therefore, the temperature of a thin circular region a–$r < 3$ μm of water droplets is not retrieved in the present paper.

In the case of observation in parallel rays (i.e. from the distance much greater than the droplet size), the following relation is true for the spectral radiative flux from a circular element of the opaque droplet surface:

$$q_\lambda(r) = \pi\varepsilon_\lambda(\mu)B_\lambda(T_d(r)) \quad \mu = \sqrt{1-\bar{r}^2} \qquad (7)$$

where $\bar{r}$ is the current relative radius of the circular element at the visible flat projection of the spherical droplet surface and T_d is the temperature of the droplet surface. The measured integral (over the spectrum) radiative flux is calculated as follows:

$$q_m(r) = \int_{\lambda_1}^{\lambda_2} \Phi(\lambda)F(\lambda)q_\lambda(r)d\lambda \qquad (8)$$

where λ_1 and λ_2 are the boundaries of the wavelength range, $\Phi(\lambda)$ is the spectral sensitivity of the device, $F(\lambda)$ is the spectral transmittance of the infrared filter.

Finally, the integral equation for the temperature profile to be determined is as follows:

$$q_m(r) = \pi\int_{\lambda_1}^{\lambda_2} \Phi(\lambda)F(\lambda)\varepsilon_\lambda(\mu)B_\lambda(T_d(r))d\lambda \qquad (9)$$

In the case of normal measurements for the flat water surface, one can obtain the simpler equation instead of (9):

$$q_{m,n}(r) = \pi\int_{\lambda_1}^{\lambda_2} \Phi(\lambda)F(\lambda)\varepsilon_{\lambda,n}B_\lambda(T_s(r))d\lambda \qquad (10)$$

Eq. (10) is used to calibrate the infrared camera.

3. Experimental procedure and primary results of infrared measurements

The experimental setup including the Teflon cuvette used to generate the droplet cluster is schematically presented in Fig. 4. The heater rod of diameter 1 mm and the length of 6.8 mm was made of neodymium. This rod was glued flush into the Teflon disk of thickness 1.8 mm and diameter 10 mm. Electric heating of a thin nichrome wire wound on the rod was used. The clearance between the disk and the bottom of cuvette was filled with epoxy resin.

The infrared camera FLIR SC 5600 equipped with a triangle and G3 F/3.0 Macro lens was used to obtain images of both the droplet

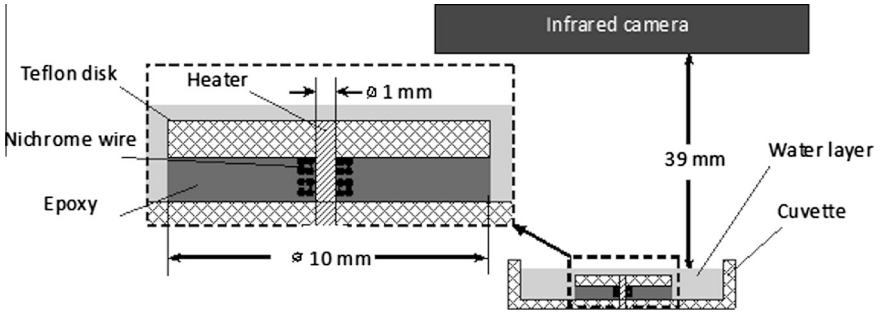

Fig. 4. Schematic of experimental setup for infrared measurements.

cluster and water layer under the cluster. The resolution of images was 640 × 512 pixels at the pixel size of 5 × 5 μm. It should be noted that image size is not so small because of 15 μm pitch detector. Therefore, the diffraction limitation is not important in our measurements. Fortunately, additional measurements at not so small pixel size showed that the experimental data in this particular case are close to be correct. The wavelength range of infrared camera from 2.5 to 5.1 μm is too wide for the measurements in the present study. Therefore, an additional narrow-band interference filter was used with the camera. The resulting spectral characteristics of the device are presented in Fig. 5. It is clear that the wavelength interval of $2.8 < \lambda < 3.3$ μmin the integral Eqs. (9) and (10) is sufficiently representative. In other words, one can use the values of $\lambda_1 = 2.8$ μm and $\lambda_2 = 3.3$ μm in subsequent calculations. Moreover, the spectral dependence of the product $\Phi \cdot F$ is controlled mainly by the filter spectral transmittance $F(\lambda)$.

Before the measurements, distilled and deionized water was poured into the cuvette with the use of stepper pipette. The initial thickness of water layer above the Teflon disk was about 300 μm. Some micro admixtures of surface-active substances do not produce unfavorable thermocapillary flows known as the Plateau–Marangoni–Gibbs effect on water surface [35].

Note that both Teflon and water are semitransparent in the near-infrared. As a result, a part of thermal radiation emitted by nichrome wire propagates towards the cluster. Fortunately, this radiation is outside the absorption band of water and has no effect on both heating the levitating water droplets and measurements of the camera equipped by the narrow-band filter.

Initially, the electric power was gradually increased up to the beginning of water boiling just at the metal heater surface. The value of this electric power was about 0.6 W. After that, the power was decreased by about one percent and it was kept constant during the measurements. This procedure leads to almost the maximum temperature of water surface without any bubbles which may disturb the generated droplet cluster. The periodic growth of droplet clusters containing from one to three cycles was observed using the video recording. The duration of one cycle was about 100–120 s. The thickness of water layer becomes smaller from cycle to cycle due to evaporation of water. As a result, the maximum temperature at the open water surface is reached and the size of generated droplets becomes greater [4,25]. To clarify a slow evolution of droplet clusters, one should recall that it is practically impossible to obtain the ideal steady-state droplet clusters. According to [25], one can say about a life cycle of a typical droplet cluster during the above specified duration with a slow growth of single droplets and their approach to the horizontal water surface.

An additional experiment was conducted to calibrate the infrared camera using thermal radiation of a hot water surface at the known temperature. Direct measurements of water temperature using a small cuvette equipped by a contact detector with absolute error about 0.02 K were used in this experiment. The water layer thickness above the detector was less that 100 μm. A combination of these two kinds of measurements enabled us to estimate an absolute experimental error of infrared measurements of water

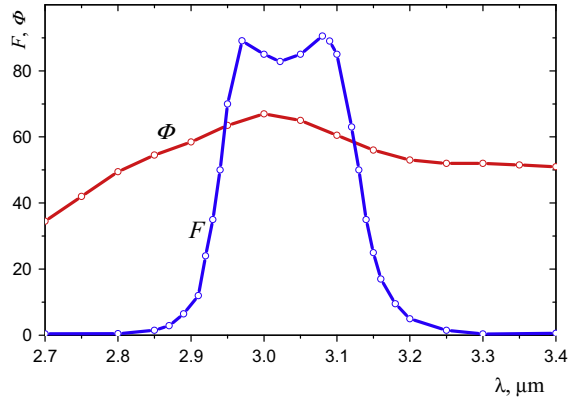

Fig. 5. Spectral sensitivity of infrared camera (Φ, in conventional units) and spectral transmittance of interference filter (F, %).

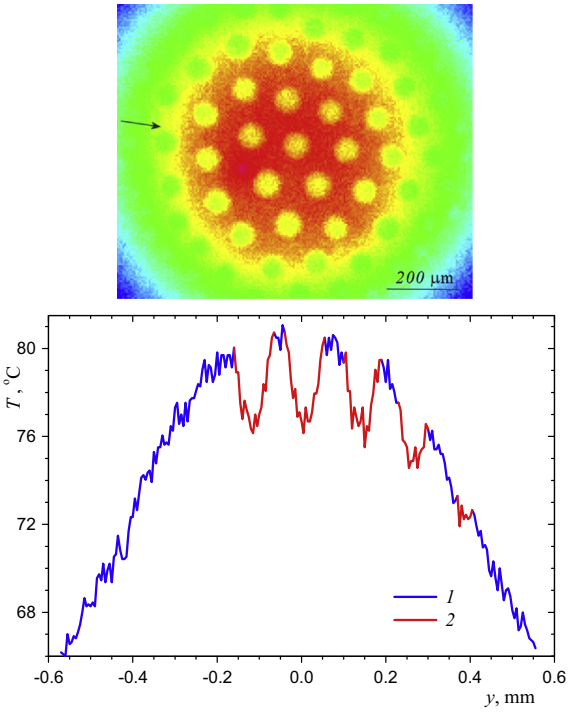

Fig. 6. Infrared image of droplet cluster and profile of brightness temperature measured in the cross section along the arrow: 1 – water layer surface, 2 – upper surface of droplets. The value of $y = 0$ corresponds to the center of droplet cluster.

temperature as about 0.16 K, which is acceptable for the regular measurements.

A typical infrared image of both the surface of water layer and the upper surface of levitating droplets is presented in Fig. 6. The profile of apparent (brightness) temperature in the cross section marked by an arrow is shown on another panel of the same figure. The coordinate y is measured from the center of heater. One can see that the heated region is axisymmetric, the cluster size is slightly greater than the heater diameter, and the temperature of water surface under the external boundary of cluster is about 20% less than that in the central region. This decrease in the water surface temperature is explained by heat conduction along the water layer. As a result, the temperature at the cluster periphery is slightly asymmetric. Note that the measured radial variation of surface temperature of water layer can be used to formulate the boundary conditions at this surface in a computational model to be developed for complex and more detailed analysis of thermal processes around the droplet cluster.

The averaged temperature profiles based on the measurements along four diameters for every droplet are presented in Fig. 7. These temperature profiles can be treated as those obtained for the same growing droplet at different time moments. It is important that the brightness temperature at the top of every droplet coincided with the real temperature because the radiation in the normal direction is observed. It means that experimental results shown in Fig. 7 enable us to conclude that surface temperature of droplets decreases significantly from the droplet "equator" towards the upper point of the droplet. Of course, one needs in accurate identification procedure to obtain the temperature profile along the droplet surface.

4. Identification of surface temperature of water droplets

The identification problem for the droplet surface temperature $T_d(r)$ can be formulated as the following integral equation:

$$\int_{\lambda_1}^{\lambda_2} \Phi(\lambda)F(\lambda)\varepsilon_\lambda(\mu)B_\lambda(T_d(r))d\lambda = \int_{\lambda_1}^{\lambda_2} \Phi(\lambda)F(\lambda)\varepsilon_{\lambda,n}B_\lambda(T_{d,b}(r))d\lambda \quad (11)$$

where $T_{d,b}$ is the measured brightness temperature. It is assumed that the temperature field of the upper surface of a droplet is axially symmetric. It was shown in Fig. 7 that there is a small asymmetry of the measured surface temperature of water droplets. Fortunately, this effect is insignificant. Therefore, the simplest arithmetic averaging was used to consider only the radial dependence of temperature. The averaged radial profiles of brightness temperature are presented in Fig. 8. The retrieved physical temperature T_d of the same droplets is also shown in this figure. The profiles of $T_d(r)$

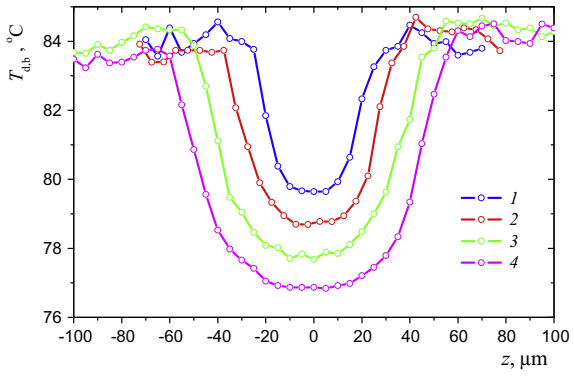

Fig. 7. The measured profiles of an apparent (brightness) temperature of different water droplets: 1 – a = 30 μm, 2 – 40 μm, 3 – 50 μm, 4 – a = 60 μm. The value of z = 0 corresponds to the center of a single droplet.

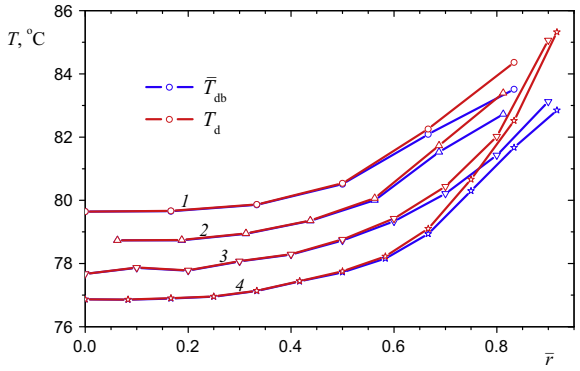

Fig. 8. The radial profiles of averaged brightness temperature $\bar{T}_{d,b}$ and the calculated profiles of physical temperature T_d of the upper surface of different water droplets: 1 – a = 30 μm, 2 – 40 μm, 3 – 50 μm, 4 – a = 60 μm.

were calculated using a simple iterative procedure to solve Eq. (11). Five iterations appeared to be quite sufficient to obtain accurately the final values of temperature. One can see in Fig. 8 that surface temperature of the peripheral region of the visible upper surface of water droplets is considerably greater than the measured brightness temperature. This effect is a result of relatively small emittance of water surface at large angles (see Fig. 3).

It is interesting that the radial temperature profiles at the upper surface of water droplets of different size are similar to each other (see Fig. 8). Moreover, the dependence of the minimum temperature at the top of a droplet on the droplet radius is almost linear. The latter is clearly illustrated in Fig. 9. Let us recall some results of similar experiments of [25], where the droplet levitation height above the water surface was obtained. Fig. 10 indicates that the heights of both the top and the bottom of a droplet decrease with the droplet size. This qualitative result is known from the early paper [2], but it is interesting to note that the tops of droplets with radius $a > 40$ μm are positioned practically at the same height. Taking into account the results presented in Fig. 9, one can conclude that temperature difference, ΔT, between the upper surface of a droplet and the steam–air flow at the same height decreases linearly with the value of a. On the other hand, the temperature difference between the bottom and the top of a growing droplet increases monotonically with the droplet radius at $a > 40$ μm. Of course, the temperature at the top of every droplet is lower than the gas temperature at the same height between the droplets. It means that the condensation of water vapor is predominant in the upper part of the droplet surface. At the same time, one can expect intense evaporation of water in the equatorial region of the droplet. One cannot exclude that the overall balance between evaporation and condensation in the case of a quasi-

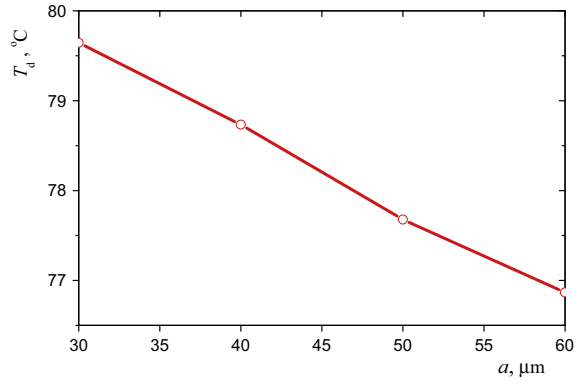

Fig. 9. Temperature at the top of droplet surface as a function of the droplet size.

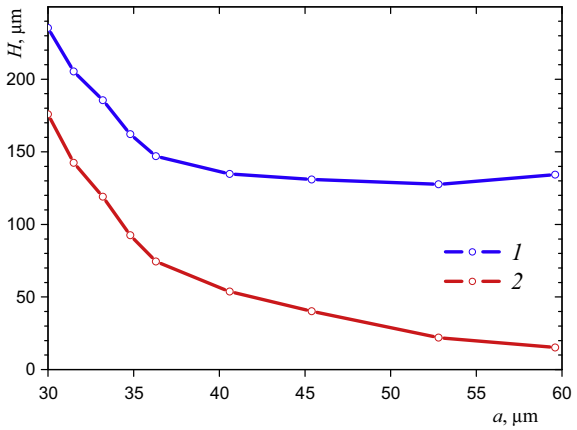

Fig. 10. The height of (1) the top and (2) the bottom of droplets levitating above the water surface.

steady droplet is reached due to additional condensation at a part of the bottom surface of the droplet. A preliminary explanation of such an effect can be based on assumption of a toroidal vortex flow in a large droplet with the upstream flow at the equator and downward flow in the central region of the droplet. Of course, a reliable flow pattern inside and outside the droplet may be and should be a subject of a separate study based on a combination of the experimental methods and detailed computational modeling.

5. Conclusion

The surface temperature of levitating water droplets was studied by using infrared measurements in the spectral absorption band of water at wavelength about 3 μm. The integral inverse problem for the temperature of the upper surface was formulated to take into account both the directional spectral emittance of the water surface and the spectral sensitivity of the detector. The iterative numerical solution of this problem showed that the real temperature of the droplet periphery is considerably greater than the measured brightness temperature. The experiments for the same droplet cluster arising over the heated water showed that the minimum temperature takes place at the top of the droplet and this temperature decreases linearly with the droplet size. The data obtained for both the temperature profile of water layer under the cluster and the temperature of the upper surface of droplets of different size are expected to be useful for validation of computational models to be developed for quasi-steady droplet clusters.

Conflict of interest

There is no conflict of interest.

Acknowledgment

The authors are grateful to the Russian Foundation for Basic Research (RFBR-Russia) for the financial support of the present study (Grants Nos. 13-08-00022-a and 15-08-00248-a).

References

[1] A.A. Fedorets, Droplet cluster, JEPT Lett. 79 (8) (2004) 372–374.
[2] A.A. Fedorets, On the mechanism of non-coalescence in a drop cluster, JEPT Lett. 81 (9) (2005) 437–441.
[3] A.A. Fedorets, Application of a droplet cluster to visualize microscale gas and liquid flows, Fluid Dyn. 43 (6) (2008) 923–926.
[4] E.A. Arinstein, A.A. Fedorets, Mechanism of energy dissipation in a droplet cluster, JEPT Lett. 92 (10) (2010) 658–661.
[5] A.A. Fedorets, I.V. Marchuk, O.A. Kabov, Role of vapor flow in the mechanism of levitation of a droplet cluster dissipative structure, Tech. Phys. Lett. 37 (3) (2011) 116–118.
[6] A.A. Fedorets, I.V. Marchuk, O.A. Kabov, Coalescence of a droplet cluster suspended over a locally heated liquid layer, Interfacial Phenom. Heat Transfer 1 (1) (2013) 51–62.
[7] W. Suhr, Tröpfchenballett auf heißem Tee, PhyDid B – Didaktik der Physik – Beiträge zur DPG-Frühjahrstagung; 2014 (ISSN 2191–379 X).
[8] T. Umeki, M. Ohata, H. Nakanishi, M. Ichikawa, Dynamics of microdroplets over the surface of hot water, arXiv:1501.00523v1 [cond-mat.soft] 3 January 2015.
[9] G. Mie, Beiträge zur Optik trüben Medien, speziell kolloidaler Melallösungen, Ann. Phys. 25 (Folge 4, H. 3) (1908) 377–445.
[10] N.A. Logan, Survey of some early studies of the scattering of plane waves by a sphere, Proc. IEEE 53 (8) (1965) 773–785.
[11] H. Horvath, Gustav Mie and the scattering and absorption of light by particles: hystoric developments and basics, J. Quant. Spectrosc. Radiat. Transfer 110 (11) (2009) 787–799.
[12] M. Kerker, The Scattering of Light and Other Electromagnetic Radiation, Academic Press, New York, 1969.
[13] H.C. van de Hulst, Light Scattering by Small Particles, Dover, New York, 1981.
[14] C.F. Bohren, D.R. Huffman, Absorption and Scattering of Light by Small Particles, Wiley, New York, 1983.
[15] L.A. Dombrovsky, Radiation Heat Transfer in Disperse Systems, Begell House, New York, 1996.
[16] M.I. Mishchenko, L.D. Travis, A.A. Lacis, Scattering, Absorption, and Emission of Light by Small Particles, Cambridge Univ. Press, Cambridge (UK), 2002.
[17] L.A. Dombrovsky, D. Baillis, Thermal Radiation in Disperse Systems: An Engineering Approach, Begell House, New York, 2010.
[18] D.Q. Choudhury, P.W. Barber, S.C. Hill, Energy-density distribution inside large nonabsorbing spheres by using Mie theory and geometric optics, Appl. Opt. 31 (18) (1992) 3518–3523.
[19] N. Velesco, T. Kaiser, G. Schweiger, Computation of the internal field of a large spherical particle by use of the geometrical-optics approximation, Appl. Opt. 36 (33) (1997) 8724–8728.
[20] L.A. Dombrovsky, Thermal radiation from nonisothermal spherical particles of a semitransparent material, Int. J. Heat Mass Transfer 43 (9) (2000) 1661–1672.
[21] P. Yang, K.N. Liou, An "exact" geometric optics approach for computing the optical properties of large absorbing particles, J. Quant. Spectrosc. Radiat. Transfer 110 (13) (2009) 1162–1177.
[22] G.M. Hale, M.P. Querry, Optical constants of water in the 200nm to 200μm wavelength region, Appl. Opt. 12 (3) (1973) 555–563.
[23] V.M. Zolotarev, A.V. Dyomin, Optical constants of water in wide wavelength range 0.1 Å÷1 m, Opt. Spectrosc. 43 (2) (1977) 271–279.
[24] M. Born, E. Wolf, Principles of Optics, Seventh (expanded) Edition, Cambridge Univ. Press, New York, 1999.
[25] A.A. Fedorets, Mechanism of stabilization of location of a droplet cluster above the liquid–gas interface, Tech. Phys. Lett. 38 (11) (2012) 988–990.
[26] D.W. Mackowski, R.A. Altenkirch, M.P. Mengüç, Internal absorption cross sections in a stratified sphere, Appl. Opt. 29 (10) (1990) 1551–1559.
[27] H.M. Lai, P.T. Leung, K.L. Poon, K. Young, Characterization of the internal energy density in Mie scattering, J. Opt. Soc. Am. A: 8 (10) (1991) 1553–1558.
[28] L.A. Dombrovsky, A modified differential approximation for thermal radiation of semitransparent nonisothermal particles: application to optical diagnostics of plasma spraying, J. Quant. Spectrosc. Radiat. Transfer 73 (2–5) (2002) 433–441.
[29] L.A. Dombrovsky, M.B. Ignatiev, An estimate of the temperature of semitransparent oxide particles in thermal spraying, Heat Transfer Eng. 24 (2) (2003) 60–68.
[30] L.A. Dombrovsky, Absorption of thermal radiation in large semi-transparent particles at arbitrary illumination of the polydisperse system, Int. J. Heat Mass Transfer 47 (25) (2004) 5511–5522.
[31] L.A. Dombrovsky, T.N. Dinh, The effect of thermal radiation on the solidification dynamics of metal oxide melt droplets, Nucl. Eng. Des. 238 (2008) 1421–1429.
[32] L.A. Dombrovsky, The use of transport approximation and diffusion-based models in radiative transfer calculations, Comput. Therm. Sci. 4 (4) (2012) 297–315.
[33] J.R. Howell, R. Siegel, M.P. Mengüç, Thermal Radiation Heat Transfer, CRC Press, New York, 2010.
[34] M.F. Modest, Radiative Heat Transfer, Third ed., Academic Press, New York, 2013.
[35] L.E. Scriven, C.V. Sternling, The marangoni effects, Nature 187 (4733) (1960) 186–188.